https://doi.org/10.1016/j.jmmm.2017.09.009
This is the Pre-Published Version.

The Effect of Different Minor Additions on the Magneto-caloric Effect of FeZrB Metallic Ribbons near Room Temperature

Guo D.Q.[1], Yuan Y.D.[2] and Chan K.C.[1,*]

1. Department of Industrial and Systems Engineering, Hong Kong Polytechnic University, Hung Hom, Hong Kong, China

2. School of Materials Science and Engineering, AnHui University of Technology, Maanshan 243032, China

*Corresponding author. E-mail address: kc.chan@polyu.edu.hk

Abstract

For room-temperature magnetic refrigerators, magnetocaloric materials are critical for their performance and reliability. Among various magnetocaloric materials, Fe-based metallic glasses, especially in the FeZrB system, have been intensively studied recently due to their promising properties such as low fabrication cost and broad magnetic entropy change peak. In order to further improve the magnetocaloric effect (MCE), the influence of minor additions of Co, Er, Sm and Mn on the MCE of FeZrB-based metallic glasses was systematically investigated in this work. The composition-dependent Curie temperatures (T_C) were studied and the magnetic field-dependent MCE was investigated. In two compositions, $Fe_{88}Zr_7B_3Co_2$ and $Fe_{86}Zr_8B_4Sm_2$, it was found that their Curie temperatures were close to room temperature and the values of the refrigerant capacity and peak magnetic entropy change were larger than those reported for Fe-based metallic glass at room temperature.

© 2017. This manuscript version is made available under the CC-BY-NC-ND 4.0 license http://creativecommons.org/licenses/by-nc-nd/4.0/

Keywords: amorphous ribbons, magnetic materials, magnetocaloric effect

1. Introduction

After the discovery of the influence of an external magnetic field on the temperature of magnetic materials in 1860 [1], the magnetocaloric effect (MCE) was reported by Warburg twenty years later [2]. This effect did not attract much attention until 1976 when Brown [3] first reported that magnetic refrigeration (MR) near room temperature could be realized on the basis of the magnetocaloric effect. The advantages of MR are due to its superior performance when compared with the conventional gas compression/vaporization refrigeration technology. MR is more energy saving and is more environmentally friendly [4, 5]. MR can achieve a coefficient of performance (COP) as high as 15 as compared to 2 to 6 for conventional refrigeration methods [6]. For conventional refrigeration technology, hazardous gas is needed, which causes a serious ozone-depletion problem. Whereas no hazardous gas is required for MR, making MR much more environmentally-friendly.

In order to realize the application of room temperature magnetic refrigeration, it is critical to synthesize a working material with a magnetocaloric effect sufficiently large near room temperature. The MCE of a magnetic material can be quantified by either of the two key parameters [7]: the isothermal magnetic entropy change (ΔS_M) and the adiabatic temperature change (ΔT_{ad}). The refrigerant capacity (RC) should also be taken into account when a magnetic material is considered for MR applications. To quantify the RC, two main variables are used: the peak magnetic entropy change (ΔS_M^{peak}) and the working temperature range (ΔT)[8]. Compared with materials that undergo first-order magnetic transition with high but narrow magnetic entropy change

peaks, those that undergo second-order magnetic transition with broadened magnetic entropy change peaks are preferred. The working materials are expected to be effective in a relatively wide temperature range in order to ensure that the magnetic refrigeration system has good performance at different temperatures. Fe-based amorphous alloys with enhanced properties have attracted much attention since their first discovery in 1967 by Duwez [9-19]. Some of the properties are advantageous over other materials with regard to the MR applications, for example, broad magnetic entropy change peak resulting in high refrigerant capacity; high electric resistance and nearly zero magnetic hysteresis losses resulting in a low energy loss and the possibility of working at high frequencies; low cost resulting in lower manufacturing costs; formability over a wide compositional range resulting in easily tunable Curie temperatures (T_C) [14]. For most Fe-based amorphous materials, their Curie temperatures are much higher than room temperature. In such circumstances, the MCE of these materials under room temperature is much lower than its maximum value which peaks around (T_C). Fe-Zr-B series metallic glasses, however, are more promising candidates for the application of room temperature magnetic refrigeration due to their T_C being relatively nearer to the room temperature. The effect of elements doping on the magnetic properties of Fe-based amorphous alloys has been studied in literature [20, 21] and they show that adjusting the compositions is a feasible method to obtain materials with desired properties. In this work, different new minor additions into FeZrB systems were attempted and the effect was investigated in order to further understand the relationship between MCE and its composition.

2. Experimental details and data analysis

Based on the findings for FeZrB ternary alloys reported in the literature and from our previous work, $Fe_{88}Zr_8B_4$ (numbered as FZB001) amorphous alloy was selected as the master alloy composition for the subsequent minor additions due to its relatively large magnetic entropy change (0.884 J/kgK under 1.5 T), its Curie temperature close to room temperature (280 K) and large refrigerant capacity (106.08 J/kg under 1.5 T). Ingots of FeZrB based alloys with different minor additions (Co, Er, Sm and Mn) were prepared from raw metallic materials with purity above 99.9% (at.%). The compositions are listed in the following table.

Number	Composition	Number	Composition
FZB001	$Fe_{88}Zr_8B_4$	FZB203	$Fe_{85}Zr_8B_4Er_3$
FZB101	$Fe_{87}Zr_8B_4Co_1$	FZB301	$Fe_{87}Zr_8B_4Sm_1$
FZB102	$Fe_{86}Zr_8B_4Co_2$	FZB302	$Fe_{86}Zr_8B_4Sm_2$
FZB103	$Fe_{88}Zr_7B_4Co_1$	FZB303	$Fe_{85}Zr_8B_4Sm_3$
FZB104	$Fe_{87}Zr_7B_4Co_2$	FZB401	$Fe_{87}Zr_8B_4Mn_1$
FZB105	$Fe_{88}Zr_8B_3Co_1$	FZB402	$Fe_{86}Zr_8B_4Mn_2$
FZB106	$Fe_{88}Zr_7B_3Co_2$	FZB403	$Fe_{85}Zr_8B_4Mn_3$
FZB107	$Fe_{87}Zr_7B_3Co_2$	FZB404	$Fe_{80}Zr_8B_4Mn_8$
FZB201	$Fe_{87}Zr_8B_4Er_1$	FZB405	$Fe_{78}Zr_8B_4Mn_{10}$
FZB202	$Fe_{86}Zr_8B_4Er_2$		

The ingots were melted repeatedly at least six times in an arc-melting machine under an argon atmosphere in order to ensure their homogeneity. A melt-spinning machine with single roller under an argon atmosphere was used to fabricate ribbons from the ingots. The dimensions of the as-spun ribbons were 0.05 mm in thickness and 1.5 mm in width. X-ray diffraction (XRD) measurement was performed with a Rigaku diffractometer with Cu-Kα radiation to check whether the as-spun ribbons were amorphous or not. The magnetic property related experiments were performed on a Quantum Design vibrating sample magnetometer (VSM). The magnetic hysteresis loops at different temperatures were obtained, with the measurements being conducted in a changing magnetic field between 0.7 T and -0.7 T, in steps of 0.007 T. The magnetization investigations were performed under temperatures from 150 K to 400 K

at 10 K per step, and in a changing magnetic field increasing from 0 to 1.5 T in 0.005 T steps. The magnetocaloric effect (MCE) of the as-spun ribbons was obtained by calculating the working temperature range (ΔT) and the peak magnetic entropy change (ΔS_M^{peak}). The magnetic entropy change (ΔS_M) was then calculated from the results of the magnetization curves under different temperatures. The detailed procedures for calculating these parameters are given in previous work[22].

3. Results and discussion

Since the experimental curves obtained for all the compositions are of similar shapes, the FZB001 and FZB201 samples were used as typical examples in this work to illustrate the results. Fig. 1a shows the XRD results of all the as-spun ribbons. All of the ribbons exhibit only a broad wave pack, around $2\theta = 45°$ and no appearance of sharp crystalline peaks, which indicates that all the as-spun ribbons are amorphous. The

patterns in Fig. 1b are the magnified XRD results of FZB001 and FZB201.

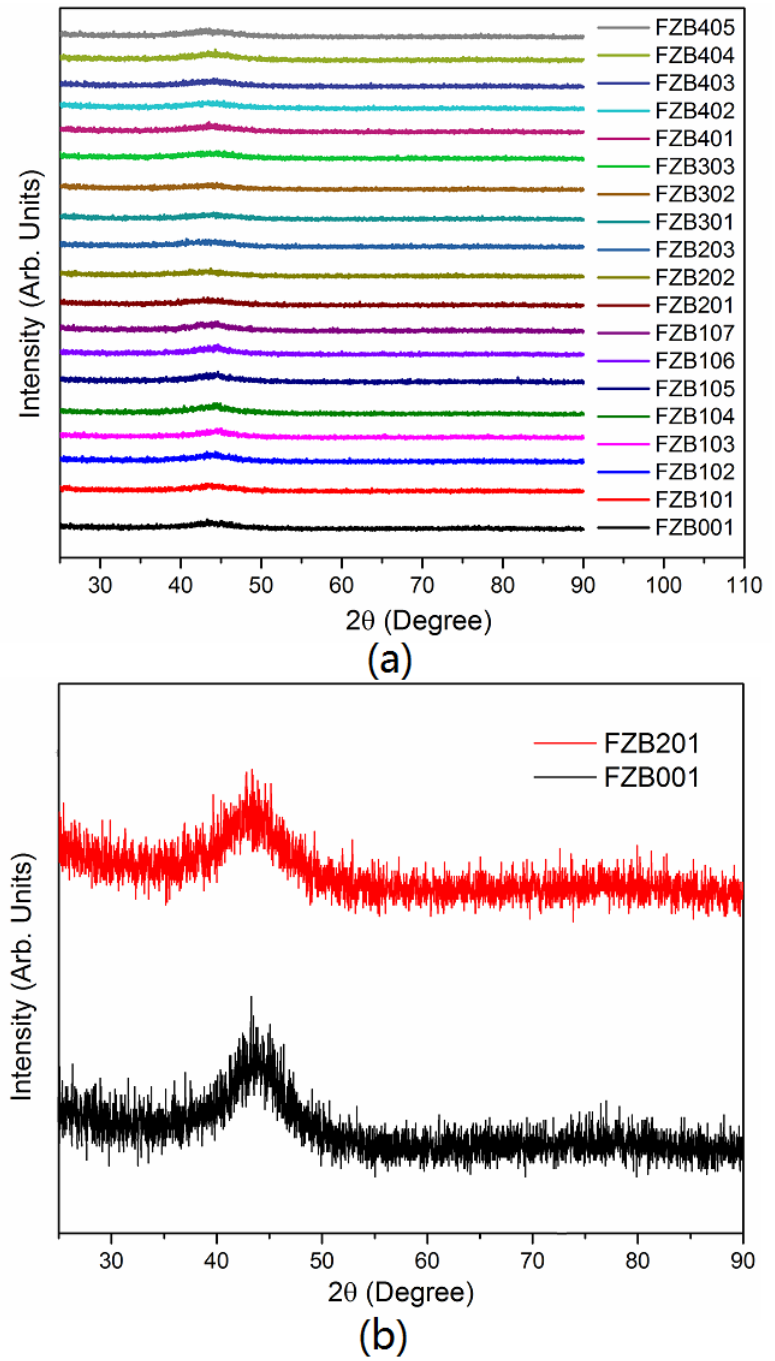

Figure 1 (a) XRD results of all as-spun ribbons (b) XRD results of FZB001 and FZB201 ribbons

Fig. 2 shows the temperature-dependent magnetization curves of the as-spun ribbons FZB001 and FZB201 for illustration. The curves were measured at different temperatures from 150 K to 400 K in 10 K steps. The applied magnetic field was 0.03 T. The inset curve is the temperature-dependent differentiation of the magnetization

with respect to the temperature (dM/dT). The Curie temperature was determined at the point where dM/dT reached its minimum value.

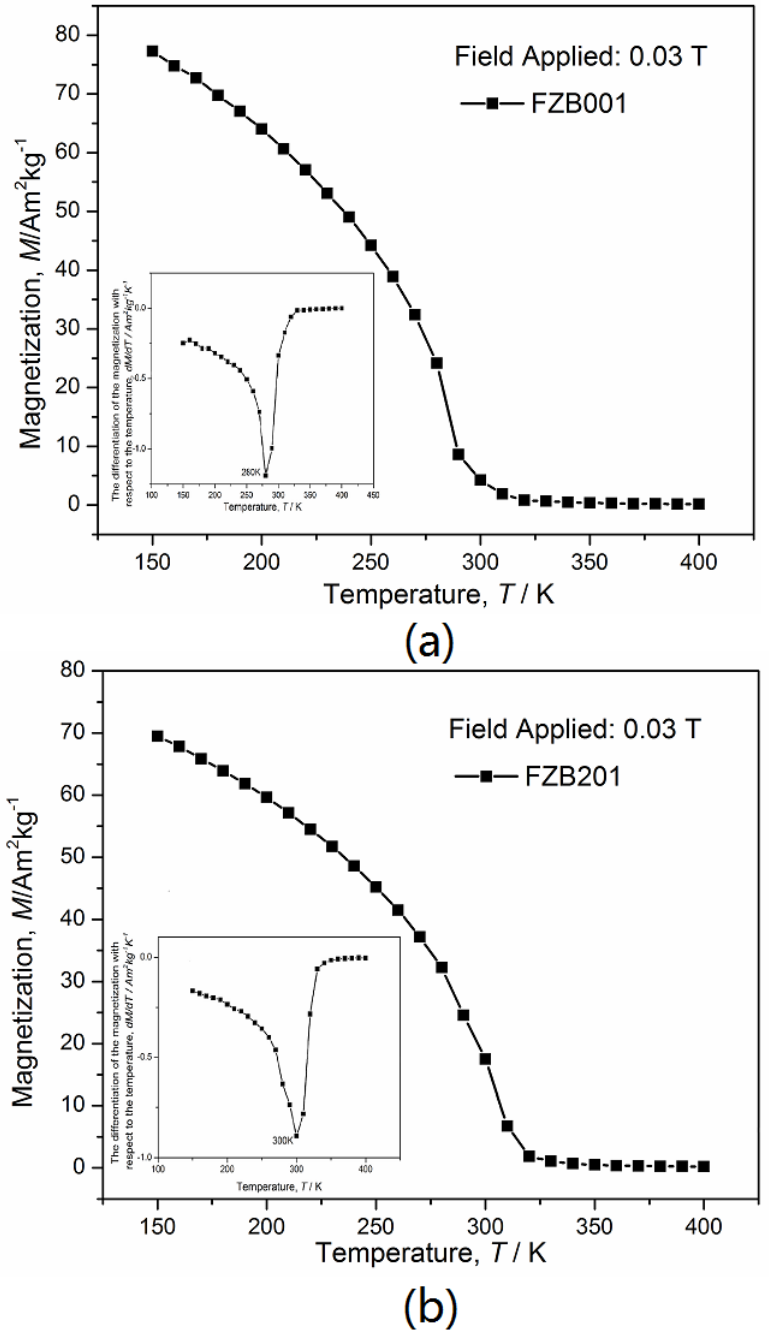

Figure 2 Temperature-dependent magnetization curves of the as-spun ribbons (a) FZB001 and (b) FZB201 ribbons. The insets are the temperature-dependent differentiation of the magnetization with respect to the temperature

A molecular theory can be applied to explain the change of the Curie temperature in different compositions[23].

$$T_C = J(r)Z_T S(S+1)/3k_B \qquad (1)$$

where T_C corresponds to the Curie temperature, $J(r)$ to the distance dependent

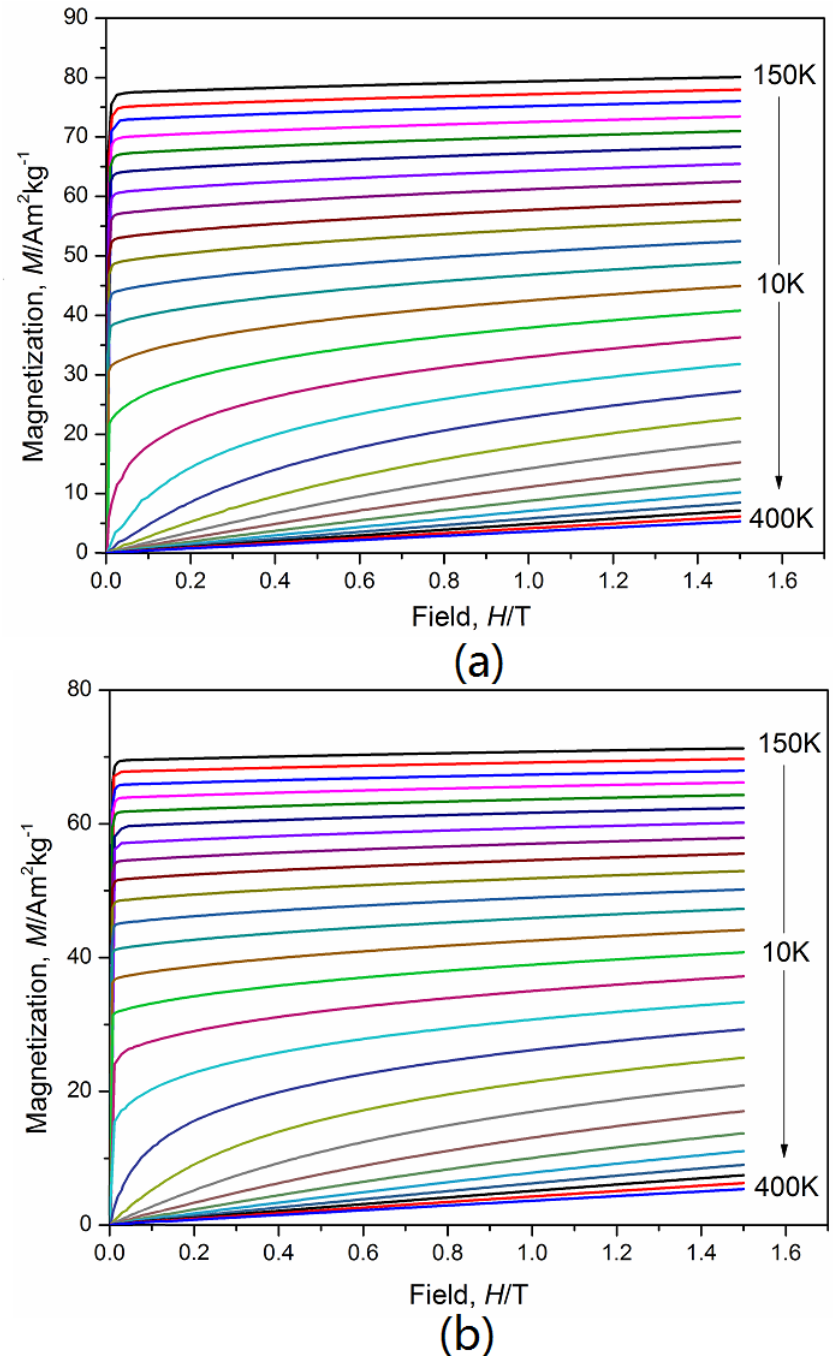

Figure 3 Isothermal magnetization curves of the as-spun ribbons (a) FZB001 and (b) FZB201 ribbons

exchange between atoms, Z_T to the coordination number of the T (T=Fe) site, S to the spin quantum number and k_B to the Boltzmann's constant. Among the four minor addition elements, the radii of the Er and Sm atoms are similar and both are much larger

than that of Fe atom; the radius of the Mn atom is slightly larger than that of the Fe atom and the radius of the Co atom is slightly smaller than that of the Fe atom. As the amount of the substitution elements increases, the number of the alloying atoms surrounding the Fe atom site increases, which increases the value of Z_T. The variation of distance (r) between the Fe atoms was investigated by simulation on the basis of a random model. For Fe atoms, $J'(r) > 0$. When Fe was substituted by 1 at.% Co, r increases from 3.49 Å to 3.59 Å. Both the increased $J(r)$ and increased Z_T work together to enlarge T_C. When Fe was substituted by 1 at.% Er or 1 at.% Mn, r decreases from 3.49 Å to 3.41 Å and 3.42 Å respectively. As the amount of Mn increased from 1 at.% to 10 at.%, r increases from 3.42 Å to 3.44 Å. When the addition amount was small, the effect of Z_T dominates T_C. Consequently, T_C tends to increase. As the amount of Mn increased, the effect of $J(r)$ became dominating and T_C was suppressed due to the fact that more antiferromagnetic coupling emerged with more short Fe-Fe bonds.

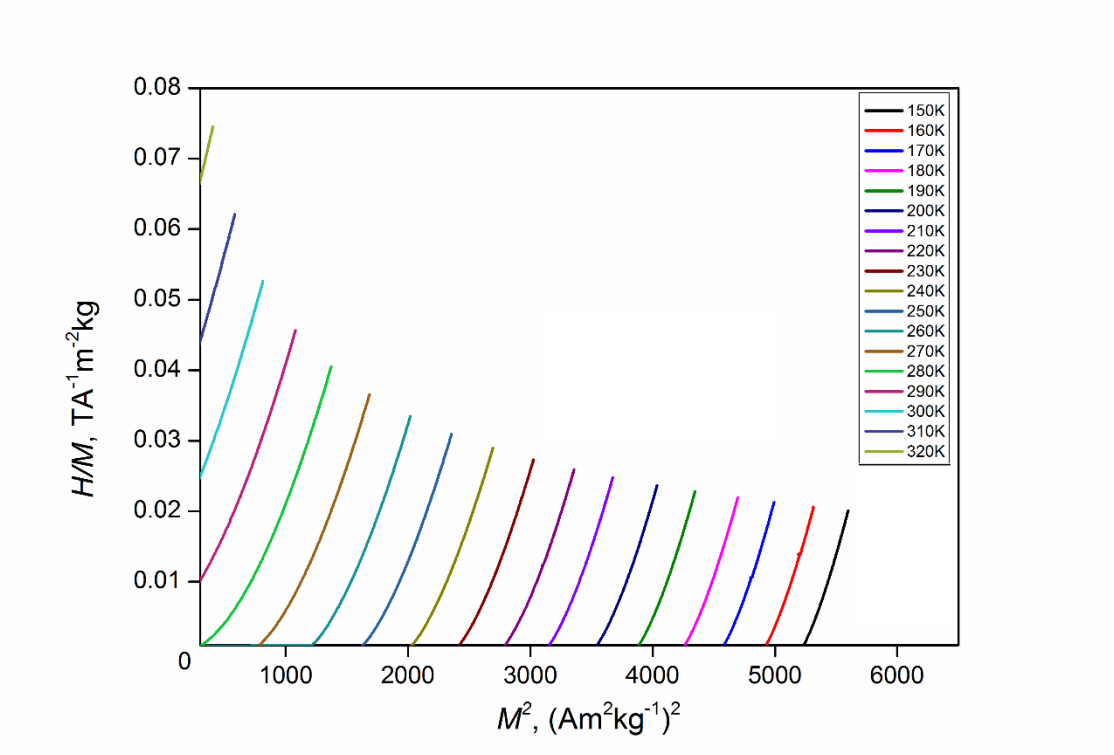

Figure 4 Arrott plot for the FZB001 samples

The isothermal magnetization curves of the as-spun ribbons FZB001 and FZB201 are presented in Fig. 3. The saturation magnetization decreases as the temperature increases.

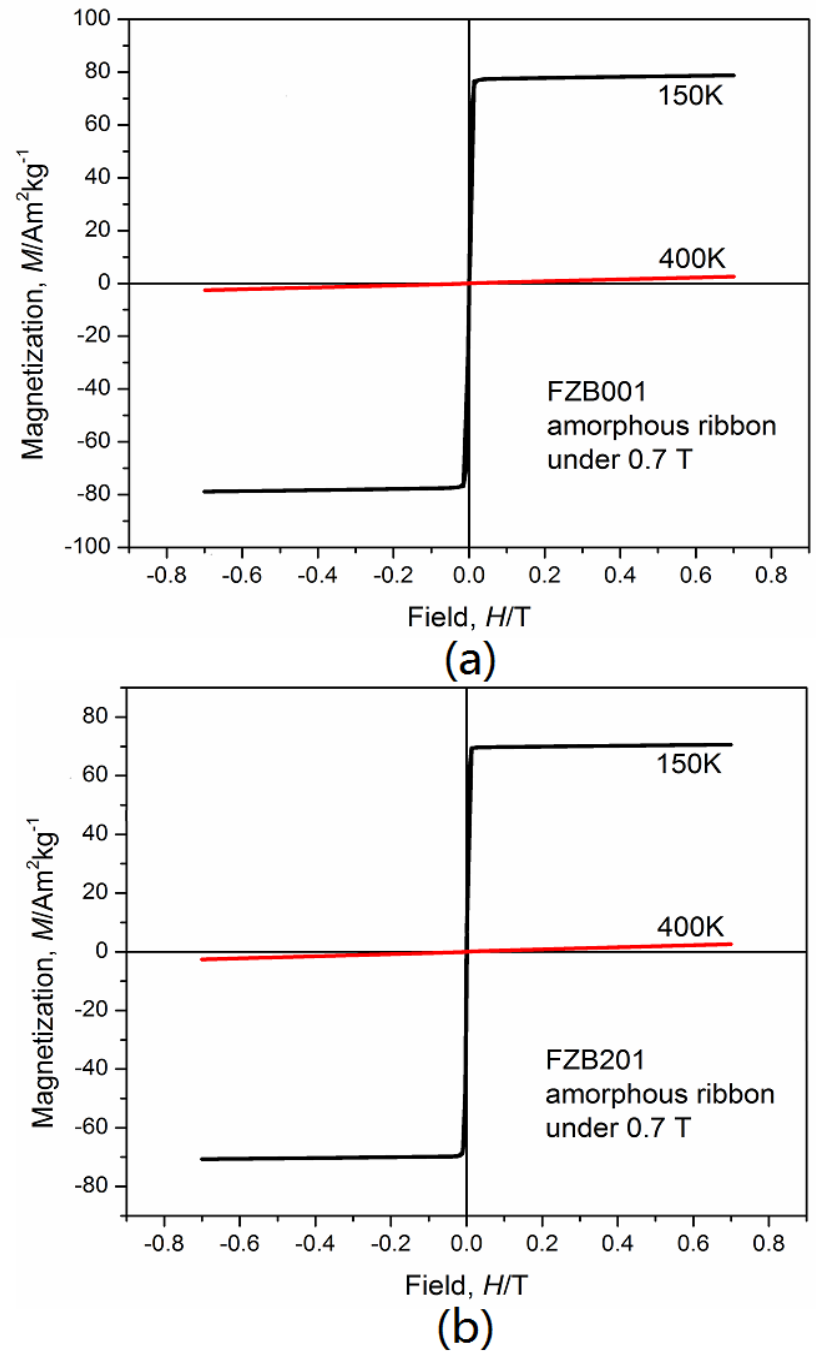

Figure 5 Magnetic hysteresis loops of the as-spun ribbons (a) FZB001 and (b) FZB201 ribbons

On the basis of the results of Fig. 3, the Arrott Plots of FZB001 were constructed in Fig. 4. According to Banerjee Criterion [24], a magnetic transition is considered as second order when the slopes of Arrott Plots are positive. The positive slopes observed in Fig.

4 illustrates that that the ribbons undergo a second order magnetic phase transition (SOMT).

Fig. 5 shows the magnetic hysteresis loops of the as-spun ribbons FZB001 and FZB201. For each ribbon, the hysteresis measurements were taken both at 150 K and 400K, corresponding to temperatures below and above the Curie temperature respectively. All the loops show nearly zero coercivity and small hysteresis, which means all the ribbons exhibit excellent soft magnetic properties.

On the basis of the magnetization results, the magnetic entropy change (ΔS_M) at different temperatures can be obtained according to $\Delta S(T,\Delta H)=\int_{H_1}^{H_2}(\partial M(T,H)/\partial T)_H\,dH$ and the temperature dependent magnetic

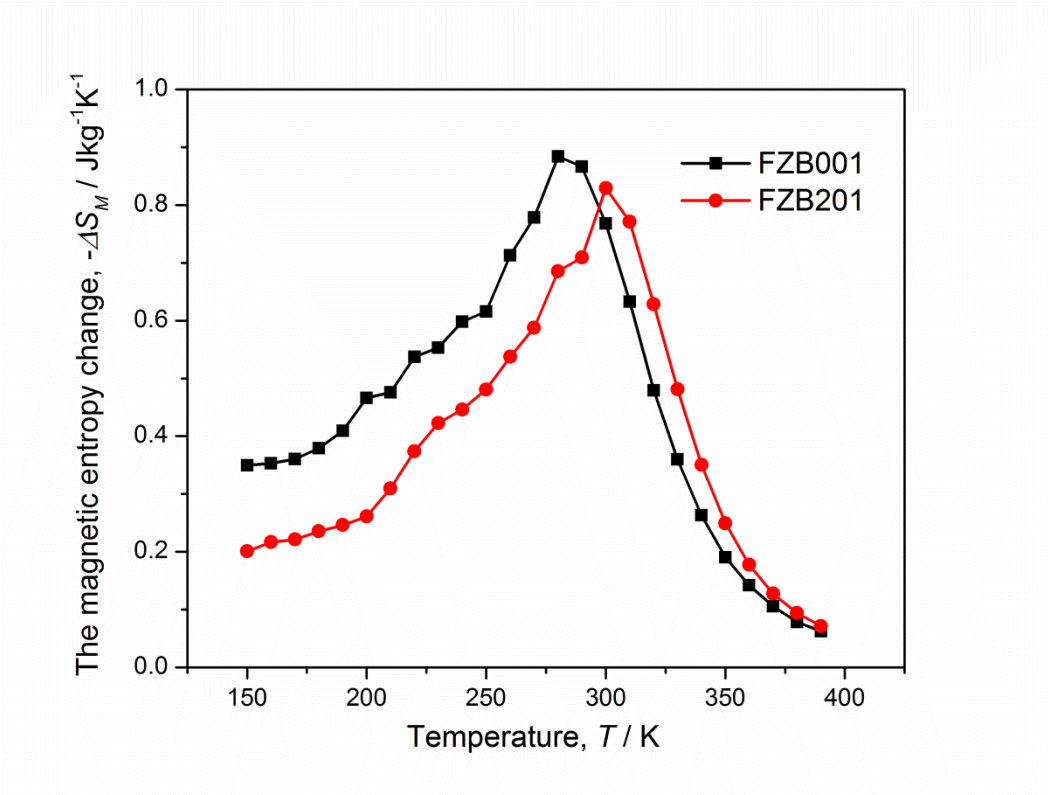

Figure 6 Temperature dependent magnetic entropy change curves of FZB001 and FZB201 ribbons under a magnetic field of 1.5 T

entropy change curves of FZB001 and FZB201 ribbons under a magnetic field of 1.5 T

are shown in Fig. 6. The shape of the curves also confirms that the ribbons undergo second order magnetic phase transition. The addition of Mn has a negative impact on the magnetic entropy change of the ribbons, while Co has a positive impact. In respect of the addition of Er and Sm, the impact was affected by the number of atoms of Er and Sm. The change of $|\Delta S_M|$ corresponded to the change of the saturation magnetization, which was also studied in literature [25].

In order to make a better comparison with results reported by other researchers, $RC(\Delta H) = |\Delta S_M^{peak}| \times \delta T_{FWHM}$ was applied to calculate the refrigerant capacity in this work. The magnetocaloric behavior of the as-spun ribbons including those investigated in this study as well as in the literature is listed in Table 1. The MCE

Table 1 The magnetocaloric effect of the magnetic materials studied in this work and reported in the literature

Nominal composition	Structure	Magnetic Field (T)	T_C (K)	δT_{FWHM} (K)	$\lvert\Delta S_M^{peak}\rvert$ (J kg^{-1}K^{-1})	RC (J kg^{-1})	Ref.
$Fe_{88}Zr_8B_4$	Amorphous	1.5	280	120	0.884	106.08	This work
$Fe_{87}Zr_8B_4Co_1$	Amorphous	1.5	320	110	0.715	78.65	This work
$Fe_{86}Zr_8B_4Co_2$	Amorphous	1.5	340	110	0.915	100.65	This work
$Fe_{88}Zr_7B_4Co_1$	Amorphous	1.5	300	130	0.672	87.36	This work
$Fe_{87}Zr_7B_4Co_2$	Amorphous	1.5	330	130	0.774	100.62	This work
$Fe_{88}Zr_8B_3Co_1$	Amorphous	1.5	300	130	0.799	103.87	This work
$Fe_{88}Zr_7B_3Co_2$	Amorphous	1.5	320	130	0.949	123.37	This work
$Fe_{87}Zr_8B_3Co_2$	Amorphous	1.5	330	140	0.945	132.6	This work
$Fe_{87}Zr_8B_4Er_1$	Amorphous	1.5	300	100	0.829	82.9	This work
$Fe_{86}Zr_8B_4Er_2$	Amorphous	1.5	300	100	0.607	60.7	This work
$Fe_{85}Zr_8B_4Er_3$	Amorphous	1.5	310	100	0.800	80	This work
$Fe_{87}Zr_8B_4Sm_1$	Amorphous	1.5	300	110	0.705	77.55	This work
$Fe_{86}Zr_8B_4Sm_2$	Amorphous	1.5	320	100	1.116	111.6	This

							work
$Fe_{85}Zr_8B_4Sm_3$	Amorphous	1.5	330	110	0.809	88.99	This work
$Fe_{87}Zr_8B_4Mn_1$	Amorphous	1.5	280	110	0.757	83.27	This work
$Fe_{86}Zr_8B_4Mn_2$	Amorphous	1.5	280	120	0.656	78.72	This work
$Fe_{85}Zr_8B_4Mn_3$	Amorphous	1.5	280	100	0.669	66.9	This work
$Fe_{80}Zr_8B_4Mn_8$	Amorphous	1.5	230	90	0.555	49.95	This work
$Fe_{78}Zr_8B_4Mn_{10}$	Amorphous	1.5	220	90	0.483	43.47	This work
$Fe_{86}Zr_9B_5$	Amorphous	1.5	330	120	1.13	135.6	[22]
$Fe_{80}Cr_4B_{10}Zr_5Gd_1$	Amorphous	1.5	360	120	0.91	110	[26]
$Fe_{75}Nb_{10}B_{15}$	Amorphous	1.5	250	190	0.60	115	[27]
$Fe_{79}Nb_7B_{14}$	Amorphous	1.5	372	N/A	1.07	N/A	[28]
$(Fe_{70}Ni_{30})_{89}Zr_7B_4$	Amorphous	1.5	342	N/A	0.70	N/A	[16]
$Fe_{64}Mn_{14}CoSi_{10}B_{11}$	Amorphous	1.5	457	N/A	0.83	N/A	[29]
$Fe_{72}Ni_{28}$	Amorphous	1.5	333	149	0.49	73	[30]
$(Fe_{85}Co_{15})_{75}Nb_{10}B_{15}$	Amorphous	1.5	440	124	0.82	102	[31]
$Gd_{55}Al_5Fe_{40}$	Amorphous	5.0	222	197	2.7	532	[32]
$Gd_{60}Fe_{20}Co_{10}Al_{10}$	Amorphous	5.0	222	167	4.4	736	[33]
$Gd_5Si_2Ge_2$	Crystalline	5.0	276	16.5	18.5	305	[34]

of ribbons in this work is generally better than that of Fe-based ribbons reported in the literature. Higher $\left|\Delta S_M^{peak}\right|$ was obtained with T_C closer to the room temperature. In the meantime, these ribbons exhibit relatively large RC.

The magnetocaloric effect obviously has a positive relation with the applied magnetic fields. In order to make a comparison between the results calculated under different external magnetic fields, the relation between magnetocaloric effect and magnetic field was investigated[35]:

$$\left|\Delta S_M(T,H)\right| \propto H^n \qquad (2)$$

where ΔS_M is the magnetic entropy change, H is the external magnetic field, T is the temperature and n is the critical exponent which is only affected by the intrinsic properties of materials themselves. The temperature dependent n value curves of the as-spun ribbon FZB001 under different magnetic fields are shown in Fig. 7. The n values at different temperature points also confirm that the ribbons exhibit soft magnetic properties: $n \approx 0.77$ at T_C; n is close to 1 at temperatures far below T_C; n is close to 2 at temperatures far above T_C.

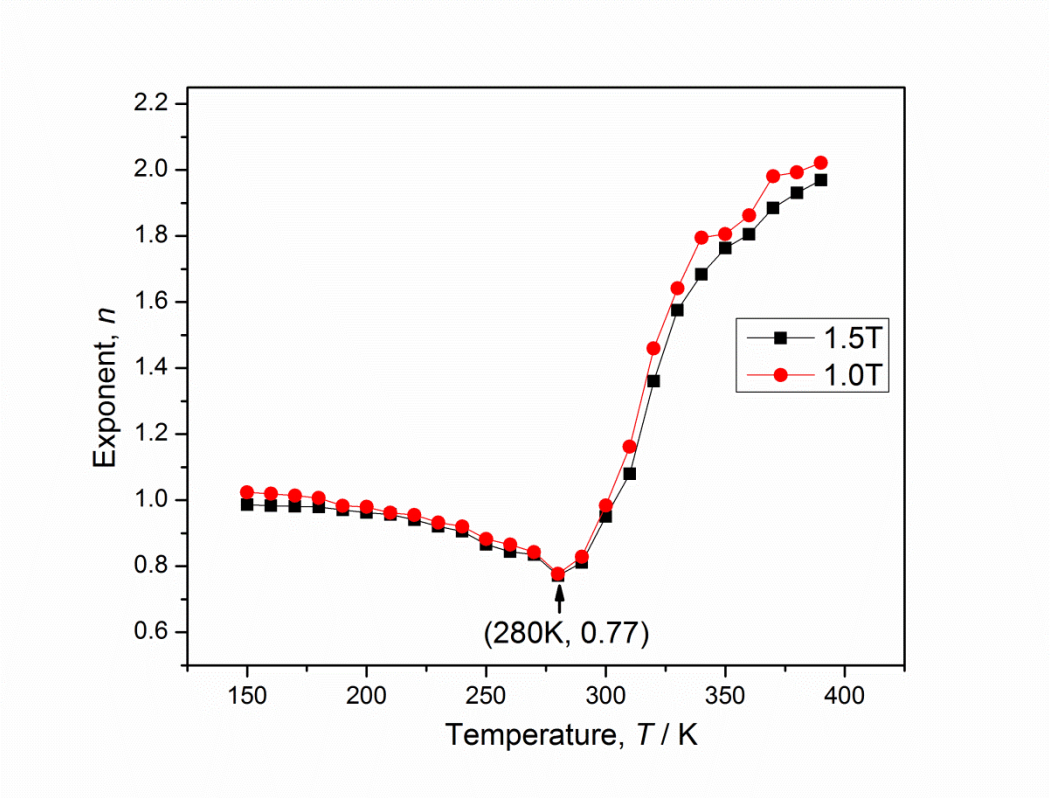

Figure 7 Temperature dependent n value curves under different magnetic fields of the as-spun ribbon FZB001

Similar to the magnetic entropy change, the refrigerant capacity is also related to the external magnetic fields and the relation was given by Franco[36] as:

$$RC \propto H^{1+1/\delta} \quad (3)$$

Detailed calculation of δ is given in previous work[22]. The result of the FZB001 sample is: $RC \propto H^{1.1595}$. With the help of Eq.(2) and Eq.(3), when the external magnetic

field changes from 1.5 T to 5.0 T, the peak magnetic entropy change of the FZB001 amorphous ribbon is 2.23 J/kgK at 280 K and the refrigerant capacity is 428.46 J/kg. Compared with the well-known $Gd_5Si_2Ge_2$ ($\left|\Delta S_M^{peak}\right|$=18.5 J/kgK, T_C=276 K and RC =305 J/kg under 5.0 T), although the $\left|\Delta S_M^{peak}\right|$ is not comparable, FZB001 exhibits almost 1.5 times of RC and its T_C is closer to room temperature.

4. Conclusions

In this work, amorphous ribbons with different minor additions (Co, Er, Sm and Mn) in the master alloy $Fe_{88}Zr_8B_4$ were fabricated. The impact of different minor additions on the magnetocaloric effect was investigated. Among all the ribbons, the $Fe_{88}Zr_7B_3Co_2$ (FZB006) ribbon exhibited the largest RC(123.37 J/kg) and $Fe_{86}Zr_8B_4Sm_2$ (FZB302) ribbon exhibited the largest $\left|\Delta S_M^{peak}\right|$(1.116 J/kgK). Both have a Curie temperature at about 320 K, which is close to room temperature. The relationship between the composition and the Curie temperature was investigated, which was determined by both the inter-atomic distances and coordination numbers. The results theoretically gave guidance in adjusting the Curie temperature of Fe-based alloys. Although the relationship between the composition and the peak magnetic entropy changes was characterized in this work, its detailed mechanism is yet to be fully understood and is worth further study.

5. Acknowledgment

This work was fully supported by the Research Committee of The Hong Kong Polytechnic University under research student account code RT4T.

References

[1] W. Thomson, "II. On the thermoelastic, thermomagnetic, and pyroelectric properties of matter," *Philosophical Magazine Series 5,* vol. 5, pp. 4-27, 1878/01/01 1878.

[2] E. Warburg, "Magnetische Untersuchungen," *Annalen der Physik,* vol. 249, pp. 141-164, 1881.

[3] G. V. Brown, "Magnetic heat pumping near room temperature," *Journal of Applied Physics,* vol. 47, pp. 3673-3680, 1976.

[4] K. Gschneidner Jr and V. Pecharsky, "Magnetocaloric materials," *Annual review of materials science,* vol. 30, pp. 387-429, 2000.

[5] K. A. GschneidnerJr, V. K. Pecharsky, and A. O. Tsokol, "Recent developments in magnetocaloric materials," *Reports on Progress in Physics,* vol. 68, pp. 1479-1539, 2005.

[6] K. A. Gschneidner and V. K. Pecharsky, "Magnetic refrigeration materials (invited)," *Journal of Applied Physics,* vol. 85, p. 5365, 1999.

[7] V. K. Pecharsky and K. A. Gschneidner, "Magnetocaloric effect and magnetic refrigeration," *Journal of Magnetism and Magnetic Materials,* vol. 200, pp. 44-56, Oct 1999.

[8] M. E. Wood and W. H. Potter, "General analysis of magnetic refrigeration and its optimization using a new concept: maximization of refrigerant capacity," *Cryogenics,* vol. 25, pp. 667-683, 1985.

[9] I. Skorvanek and J. Kovac, "Magnetocaloric behaviour in amorphous and nanocrystalline FeNbB soft magnetic alloys," *Czechoslovak Journal of Physics,* vol. 54, pp. D189-D192, 2004.

[10] F. Johnson and R. D. Shull, "Amorphous-FeCoCrZrB ferromagnets for use as high-temperature magnetic refrigerants," *Journal of Applied Physics,* vol. 99, p. 08K909, 2006.

[11] V. Franco, A. Conde, and L. F. Kiss, "Magnetocaloric response of FeCrB amorphous alloys: Predicting the magnetic entropy change from the Arrott–Noakes equation of state," *Journal of Applied Physics,* vol. 104, p. 033903, 2008.

[12] Y. K. Fang, C. C. Yeh, C. C. Hsieh, C. W. Chang, H. W. Chang, W. C. Chang, X. M. Li, and W. Li, "Magnetocaloric effect in Fe–Zr–B–M (M=Mn, Cr, and Co) amorphous systems," *Journal of Applied Physics,* vol. 105, p. 07A910, 2009.

[13] A. Makino, T. Kubota, C. Chang, M. Makabe, and A. Inoue, "FeSiBP Bulk Metallic Glasses with Unusual Combination of High Magnetization and High Glass-Forming Ability," *Materials Transactions,* vol. 48, pp. 3024-3027, 2007.

[14] P. Álvarez, J. S. Marcos, P. Gorria, L. F. Barquín, and J. A. Blanco, "Magneto-caloric effect in FeZrB amorphous alloys near room temperature," *Journal of Alloys and Compounds,* vol. 504, pp. S150-S154, 2010.

[15] J. Y. Law, V. Franco, and R. V. Ramanujan, "Influence of La and Ce additions on the magnetocaloric effect of Fe–B–Cr-based amorphous alloys," *Applied Physics Letters,* vol. 98, p. 192503, 2011.

[16] J. J. Ipus, H. Ucar, and M. E. McHenry, "Near Room Temperature Magnetocaloric Response of an (FeNi)ZrB Alloy," *Magnetics, IEEE Transactions on,* vol. 47, pp. 2494-2497, 2011.

[17] A. Waske, B. Schwarz, N. Mattern, and J. Eckert, "Magnetocaloric (Fe–B)-based amorphous alloys," *Journal of Magnetism and Magnetic Materials,* vol. 329, pp. 101-104, 2013.

[18] R. Caballero-Flores, V. Franco, A. Conde, K. E. Knipling, and M. A. Willard, "Influence of Co and Ni addition on the magnetocaloric effect in $Fe_{88-2x}Co_xNi_xZr_7B_4Cu_1$ soft magnetic amorphous alloys," *Applied Physics Letters,* vol. 96, pp. 182506-3, 2010.

[19] P. Duwez, "Amorphous Ferromagnetic Phase in Iron-Carbon-Phosphorus Alloys," *Journal of Applied Physics,* vol. 38, p. 4096, 1967.
[20] A. Zamani, R. Moubah, M. Ahlberg, H. Stopfel, U. B. Arnalds, A. Hallén, B. Hjörvarsson, G. Andersson, and P. E. Jönsson, "Magnetic properties of amorphous Fe93Zr7 films: Effect of light ion implantation," *Journal Of Applied Physics,* vol. 117, p. 143903, 2015.
[21] R. Moubah, M. Ahlberg, A. Zamani, A. Olsson, S. Shi, Z. Sun, S. Carlson, A. Hallén, B. Hjörvarsson, and P. E. Jönsson, "Origin of the anomalous temperature dependence of coercivity in soft ferromagnets," *Journal Of Applied Physics,* vol. 116, p. 053906, 2014.
[22] D. Q. Guo, K. C. Chan, L. Xia, and P. Yu, "Magneto-caloric effect of $Fe_xZr_yB_{100-x-y}$ metallic ribbons for room temperature magnetic refrigeration," *Journal Of Magnetism And Magnetic Materials,* vol. 423, pp. 379-385, 2017.
[23] R. C. O'Handley, "Physics of ferromagnetic amorphous alloys," *Journal Of Applied Physics,* vol. 62, pp. R15-R49, 1987.
[24] B. K. Banerjee, "On a Generalised Approach to First and Second Order Magnetic Transitions," *Physics Letters,* vol. 12, pp. 16-17, 1964
[25] R. Moubah, A. Boutahar, H. Lassri, A. Dinia, S. Colis, B. Hjörvarsson, and P. E. Jönsson, "Enhanced magnetocaloric properties of FeZr amorphous films by C ion implantation," *Materials Letters,* vol. 175, pp. 5-8, 2016.
[26] D. Guo, K. C. Chan, and L. Xia, "Influence of Minor Addition of Cr on the Magnetocaloric Effect in Fe-Based Metallic Ribbons," *Materials Transactions,* vol. 57, pp. 9-14, 2016.
[27] J. J. Ipus, J. S. Blazquez, V. Franco, A. Conde, and L. F. Kiss, "Magnetocaloric response of $Fe_{75}Nb_{10}B_{15}$ powders partially amorphized by ball milling," *Journal of Applied Physics,* vol. 105, pp. 123922-6, 2009.
[28] S.-G. Min, K.-S. Kim, S.-C. Yu, and K.-W. Lee, "The magnetization behavior and magnetocaloric effect in amorphous Fe–Nb–B ribbons," *Materials Science & Engineering A,* vol. 449-451, pp. 423-425, 2007.
[29] J. H. Lee, S. J. Lee, W. B. Han, H. H. An, and C. S. Yoon, "Magnetocaloric effect of $Fe_{64}Mn_{15-x}Co_xSi_{10}B_{11}$ amorphous alloys," *Journal of Alloys and Compounds,* vol. 509, pp. 7764-7767, 2011.
[30] H. Ucar, J. J. Ipus, V. Franco, M. E. McHenry, and D. E. Laughlin, "Overview of Amorphous and Nanocrystalline Magnetocaloric Materials Operating Near Room Temperature," *Jom,* vol. 64, pp. 782-788, 2012.
[31] J. J. Ipus, J. S. Blázquez, V. Franco, and A. Conde, "Influence of Co addition on the magnetic properties and magnetocaloric effect of Nanoperm $(Fe_{1-x}Co_x)_{75}Nb_{10}B_{15}$ type alloys prepared by mechanical alloying," *Journal of Alloys and Compounds,* vol. 496, pp. 7-12, 2010.
[32] Q. Dong, B. Shen, J. Chen, J. Shen, F. Wang, H. Zhang, and J. Sun, "Large magnetic refrigerant capacity in $Gd_{71}Fe_3Al_{26}$ and $Gd_{65}Fe_{20}Al_{15}$ amorphous alloys," *Journal of Applied Physics,* vol. 105, pp. 053908-053908-4, 2009.
[33] B. Schwarz, B. Podmilsak, N. Mattern, and J. Eckert, "Magnetocaloric effect in Gd-based $Gd_{60}Fe_xCo_{30-x}Al_{10}$ metallic glasses," *Journal of Magnetism and Magnetic Materials,* vol. 322, pp. 2298-2303, 2010.
[34] V. K. Pecharsky and J. K. A. Gschneidner, "Giant Magnetocaloric Effect in $Gd_5(Si_2Ge_2)$," *Physical Review Letters,* vol. 78, pp. 4494-4497, 1997.
[35] V. Franco, A. Conde, J. M. Romero-Enrique, and J. S. Blázquez, "A universal curve for the magnetocaloric effect: an analysis based on scaling relations," *Journal of Physics: Condensed Matter,* vol. 20, p. 285207, 2008.
[36] V. Franco and A. Conde, "Scaling laws for the magnetocaloric effect in second order phase transitions: From physics to applications for the characterization of materials," *International Journal of Refrigeration,* vol. 33, pp. 465-473, 2010.